Facies (2012) 58:279–296
DOI 10.1007/s10347-011-0279-8

ORIGINAL ARTICLE

A delayed carbonate factory breakdown during the Tethyan-wide Carnian Pluvial Episode along the Cimmerian terranes (Taurus, Turkey)

Susanne Lukeneder · Alexander Lukeneder · Mathias Harzhauser · Yeşim İslamoğlu · Leopold Krystyn · Richard Lein

Received: 23 May 2011 / Accepted: 3 November 2011 / Published online: 14 December 2011

Abstract This paper presents a detailed facies analysis and paleo-depth reconstruction of a latest Early Carnian platform drowning-sequence from the Anatolian terrane (Turkey, Taurus Mountains). A total of eight sedimentary microfacies zones were recorded. An open platform margin passes through a deeper shelf margin setting into a basinal environment influenced by more open-marine conditions. The analysis demonstrates an unexpected, pure carbonate depositional system through the so-called Carnian Pluvial Episode (CPE), which has previously been associated with dramatic climate changes throughout the Tethys region. One main finding, based on sedimentological and paleontological analyses, is a much later drowning of the carbonate platforms in Turkey than in other places. The termination of the Kartoz platform postdates the onset of the CPE in the western Tethys by one ammonite zone, corresponding to about 2 million years. The distinctly earlier demise of (north)western Tethyan carbonate platforms and reefs points to a diachrony of this event throughout the Tethys. The decline of carbonate productivity clearly occurs earlier at higher paleolatitudes and later in equatorial areas. Interpreting the CPE as the result of a global or at least Tethys-wide climatic event is therefore highly ambiguous. The described facies changes at Aşağiyaylabel probably mirror different coupling effects and, only minimally, the Tethyan-wide climate changes during the Carnian Pluvial Episode.

Keywords Facies change · Carnian Pluvial Episode · Late Triassic · Tethys realm · Taurus Mountains · Turkey

S. Lukeneder (✉) · A. Lukeneder · M. Harzhauser
Museum of Natural History Vienna, Vienna, Austria
e-mail: susanne.lukeneder@nhm-wien.ac.at

Y. İslamoğlu
MTA - Mine Research Department, Ankara, Turkey

L. Krystyn
Department of Palaeontology, University of Vienna, Vienna, Austria

R. Lein
Department of Geodynamics and Sedimentology, University of Vienna, Vienna, Austria

Introduction

In Europe, the platform and reef demise during the Early Carnian is known as the Carnian Crisis or the Carnian Pluvial Episode (Simms and Ruffell 1989). According to Kozur and Bachmann (2010), this was a longer and multi-phased process rather than a single event. We therefore prefer the original term Carnian Pluvial Episode (CPE) (Simms and Ruffell 1989) instead of "Middle Carnian Pluvial Event" (Hornung and Brandner 2005), which corresponds to the MCWI (= Middle Carnian Wet Intermezzo) of Kozur and Bachmann (2010). This episode is characterized by abundant siliciclastics transported by large rivers from the Baltic Craton towards the northwestern branch of the Tethys. This resulted in a collapse of the reef and carbonate platform systems and an accumulation of siliciclastic material in basinal areas and on the shelves (Tollmann 1976; Aigner and Bachmann 1992; Hornung and Brandner 2005). This involved an almost complete breakdown of reef ecosystems, combined with an abrupt decline of carbonate production (e.g., Riedel 1991; Rüffer and Zamparelli 1997; Flügel and Senowbari-Daryan 2001; Keim et al. 2001). The sudden increase in siliciclastic input (Reingraben Event) explains the breakdown of the carbonate factory (Hornung and Brandner 2005). The "mid-Carnian Event" (after Hallam

1996; Hallam and Wignall 1997) is one of the five main extinction events in the Triassic with global relevance. Palynological investigations by Hochuli and Frank (2000) date the siliciclastic interval of the Cluozza Member (Eastern Swiss Alps) as Lower Carnian (Julian) and indicate humid conditions caused by a major transgressive phase. Gianolla et al. (1998) correlated the flooding event of the first Carnian sequence with the Ladinian/Carnian boundary (Gianolla et al. 1998; Hochuli and Frank 2000). These humid environmental conditions during the latest Julian and earliest Tuvalian were documented by palynological investigations in the Carnian of the Cave del Predil area (Julian Alps, NE Italy) (Roghi 2004). The "mid-Carnian Event" is the nominal equivalent of the so-called "Reingraben turning point" of Schlager and Schöllnberger (1974), reflected in biofacies, lithofacies, and in evolutionary events mirrored in all facies belts of the entire NW Tethyan continental margin (Hornung and Brandner 2005).

The studied sequence at Aşağiyaylabel starts with shallow-water limestones of the Kartoz Formation, with thick-shelled bivalves and corals. This phase ends with a corroded and iron oxide-stained dissolution surface, pointing to subaerial exposure. The Kartoz Formation is drowned and disconformably overlain by deeper-water, hemipelagic, black limestones of the Kasımlar Formation with a thin level of ammonite floatstones (*Orthoceltites* beds) at the base. This is followed by a thick slump breccia containing up to meter-sized patch reef blocks together with comparably small ammonite coquinas and filament limestone components. The Early to Late Carnian boundary is marked by a change to grey limy marlstones, with rare ammonite- and pelagic-bivalve-bearing layers passing upwards into a thick pile of sterile dark shale with thin silty and rare siliciclastic interbeds. Microfacies analysis shows the Carnian depositional system at Aşağiyaylabel to be an intra-shelf platform environment grading upwards into deeper zones influenced by pelagic conditions.

The main topic at Aşağiyaylabel was originally to determine the environmental conditions and the original paleodepth of the Carnian ammonite mass-occurrence. However, a delayed carbonate productivity crisis at Aşağiyaylabel versus in western Tethys sections casts doubt on the Carnian event hypothesis and sparked the present facies study.

The CPE is dated to the upper *Trachyceras aonoides* and the entire *Austrotrachyceras austriacum* ammonite zones (Fig. 1b) with a duration of ca. 3.5 m.y. according to Gradstein et al. (2004) and Ogg et al. (2008) (based on the involved ammonite zones). This is distinctly longer than the 1 m.y. duration assumed by Hornung et al. (2007a, b). Platform drowning and change to argillaceous sedimentation, however, occurred much later in Aşağiyaylabel, i.e., close to or at the top of the *Austriacum* Zone. The main cause of the CPE is still under discussion (Kozur 1989; Simms and Ruffell 1989; Simms et al. 1995; Keim et al. 2001; Hornung and Brandner 2005; Rigo et al. 2007). Global warming, combined with enhanced humidification during the Early Carnian, probably triggered a climate change during that time interval (Hornung et al. 2006, 2007a, b; Hornung 2008).

Geography and geological setting

The Aşağiyaylabel section is located in southwest Turkey, about 90 km northeast of Antalya and approximately 70 km southeast of Isparta (Fig. 2). Aşağiyaylabel is accessible from the two major cities of the region, Eğirdir and Beyşehir, located 50 km and 40 km away, respectively. The locality adjoins the small village Aşağiyaylabel (1,000 m above sea-level) on the northern slope of an east to west-trending ridge between 1,050 m and 1,100 m at N 37°33′05″ and E 31°18′14″. The former name of Aşağiyaylabel was Kartoz, after which the Kartoz Formation was named (Dumont 1976; Gindl 2000). Geologically, the area is located on the Anamas Dağ carbonate platform or Anamas-Akseki Autochthonous. The Anamas Dağ is part of the so-called Taurus-Platform-Units between the Antalya Suture in the south and the Izmir-Ankara Suture in the north, south of the Isparta Angle (Robertson 1993; Senel 1997; Andrew and Robertson 2002; Robertson et al. 2003). The Anamas-Akseki Autochthonous (= Karacahisar-Autochthonous) includes Middle to Late Triassic limestones, marlstones and shales of up to 500 m thickness (Gindl 2000). The geology of southwestern Turkey and the Anamas Dağ carbonate platform has been extensively investigated by Özgül and Arpat (1973), Dumont and Kerey (1975), Monod (1977), Poisson (1977), Gutnic et al. (1979), Robertson (1993, 2000), Senel (1997), and Robertson et al. (2003).

The paleogeographic domain of the Anatolian System (Taurus Mountains, Turkey) was characterized during Triassic times by microplates located in the middle of the western Tethys Ocean. The investigated sequence was deposited in an intra-shelf basin of equatorial paleolatitude at the western end of the "Cimmerian terranes" or "Cimmerian blocks" (Şengör et al. 1984; Dercourt et al. 1993, 2000; Gindl 2000; Scotese et al. 1989; Scotese 1998, 2001; Stampfli and Borel 2002; Stampfli et al. 2002) (Fig. 1a). This area was located between the "old" Paleotethys in the north and the Neotethys in the south during the Late Triassic (Carnian, 228–216.5 Ma; Gindl 2000; Gradstein et al. 2004). While the Paleotethys Ocean underwent subduction along the southern margin of Eurasia, the young Neotethys Ocean (southern branch of Neotethys, sensu Şengör and Yılmaz 1981) was widened between the African continent and the Cimmerian terranes, which consisted of Turkey,

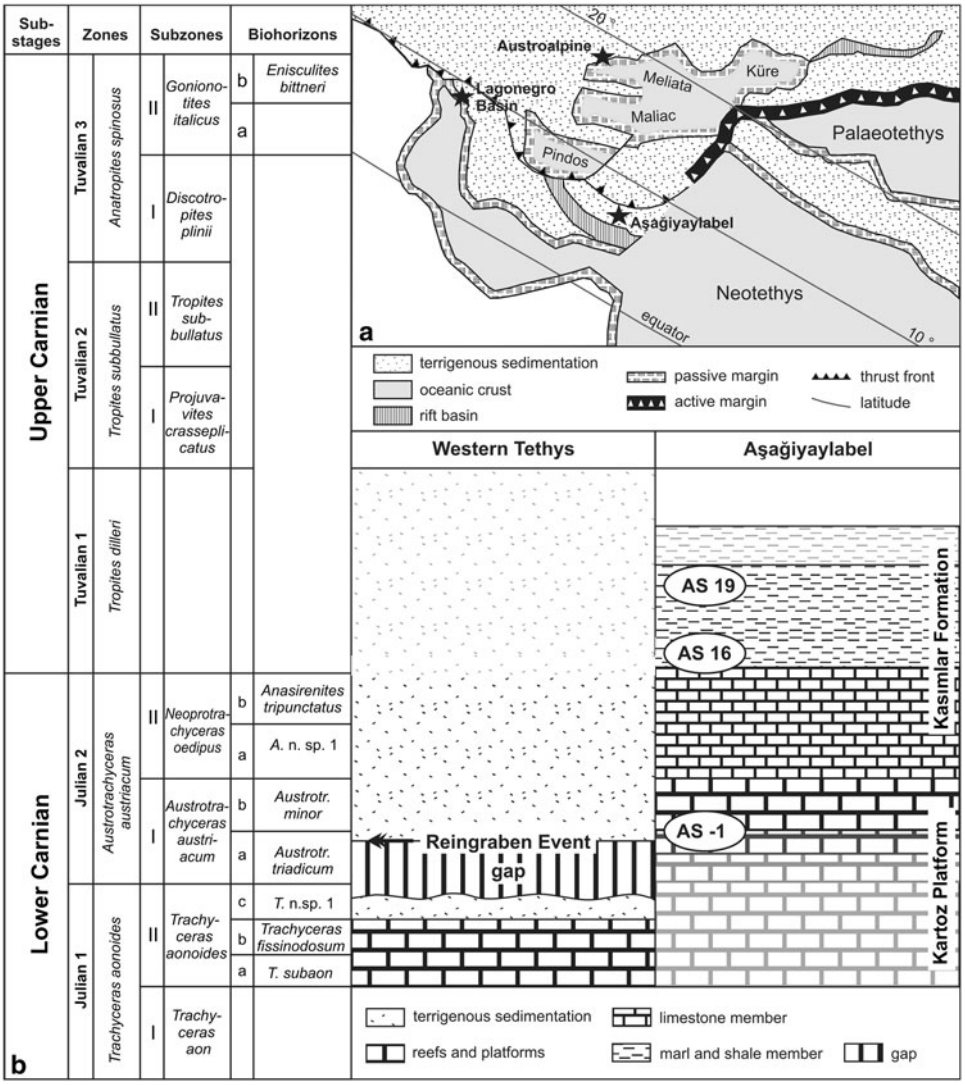

Fig. 1 **a** Paleogeographic position of the Taurus and Anatolian terranes during the Upper Triassic (after Stampfli et al. 2002) with marked position of Aşağiyaylabel, the Lagonegro Basin, and the Austroalpine region. The paleolatitude is based on Moix et al. (2008), but contrasts with Muttoni et al. (2004). **b** Late Triassic time-scale accompanied by depositional areas of the western Tethys and the lithological sequence from Aşağiyaylabel

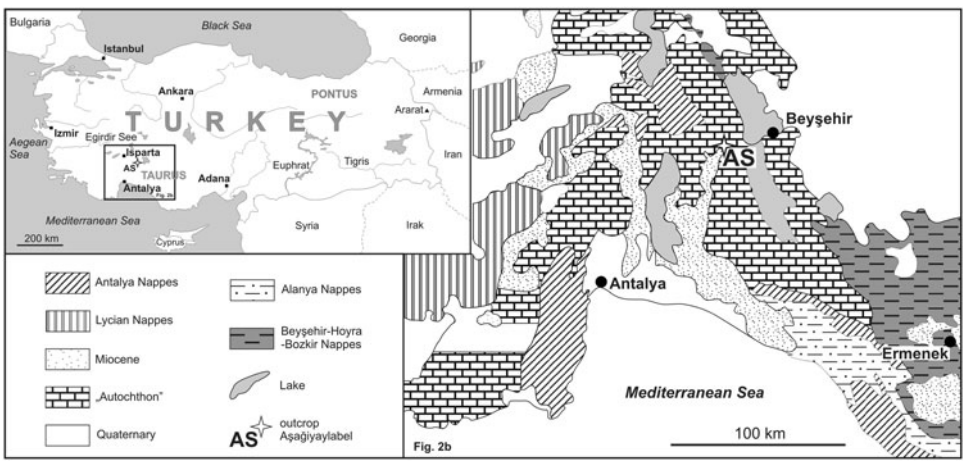

Fig. 2 Geography and geology of the investigated area with indicated position of the section Aşağiyaylabel in the Taurus Mountains (Anatolia, Turkey). Tectonic map modified after Gallet et al. (2007)

Iran, Afghanistan, Tibet, and Malaysia (Golonka 2004). In the north of these Cimmerian terranes, the İzmir-Ankara Ocean (northern branch of the Neotethys, sensu Şengör and Yılmaz 1981) and the "old" Paleotethys were still open to the east (Tekin et al. 2002; Golonka 2004; Tekin and Göncüoğlu 2007; Göncüoğlu et al. 2010).

The Triassic sequence of Aşağiyaylabel starts with an angular unconformity above Carboniferous rocks (Dumont 1976; Gindl 2000). The main formations are the Middle to Late Triassic Kartoz Formation (Early Carnian) and the Kasımlar Formation (latest Early Carnian to Late Carnian). The Kartoz Formation consists of shallow-water platform carbonates with thick-shelled bivalves (megalodonts) and corals. In contrast, the overlying Kasımlar Formation starts disconformly (e.g., hiatus) with an 8-m-thick pile of deeper-water limestones; this passes via another 12 m of marlstones into shales (Fig. 3). The section is dated based on conodonts, ammonites, and halobiids; their detailed age assignment follows Krystyn et al. (2002) and Gallet et al. (2007). The strata dip approx. 45° towards northeast.

Fig. 4 Detailed views of the section at Aşağiyaylabel. Kartoz Formation: **a** As −1 to As 0, bioclastic bafflestones with abundant in situ corals (*thick whitish structure*); Kasımlar Formation: **b** As 3 to As 5, bioclastic floatstones with abundant ammonites (*Orthoceltites*) and halobiid shells accompanied by rare gastropods. **c** As 9+3 m, thick-bedded debris flow deposits with intra- and extraclast breccias, comprising Cipit boulders, up to meter-sized patch reef blocks, small ammonite coquinas and filament components. **d** As 13, wavy bedded peloidal filament-packstones, with bioturbated matrix, intercalated by residual sediments containing halobiid bivalves, sponge spicules, radiolaria, and planktic crinoids. **e** As 14 to As 15, transition from Julian limestones (As 14) to Tuvalian (As 15) peloidal pack- to grainstones at the top with sponge spicules, crinoids, and thin-shelled bivalves (halobiids). **f** As 16, fine bioclastic wackestones with strongly bioturbated matrix comprising abundant ammonites (e.g., *Neoprotrachyceras*). **g** As 18/19, slip breccia, siliciclastic breccias and "floating" blocks (up to 40 cm in diameter). **h** As 23.3 m, hundreds of meters composed of shales with intercalated siltstones. Detailed description of beds and facies in text. All *scale bars* 10 cm ▶

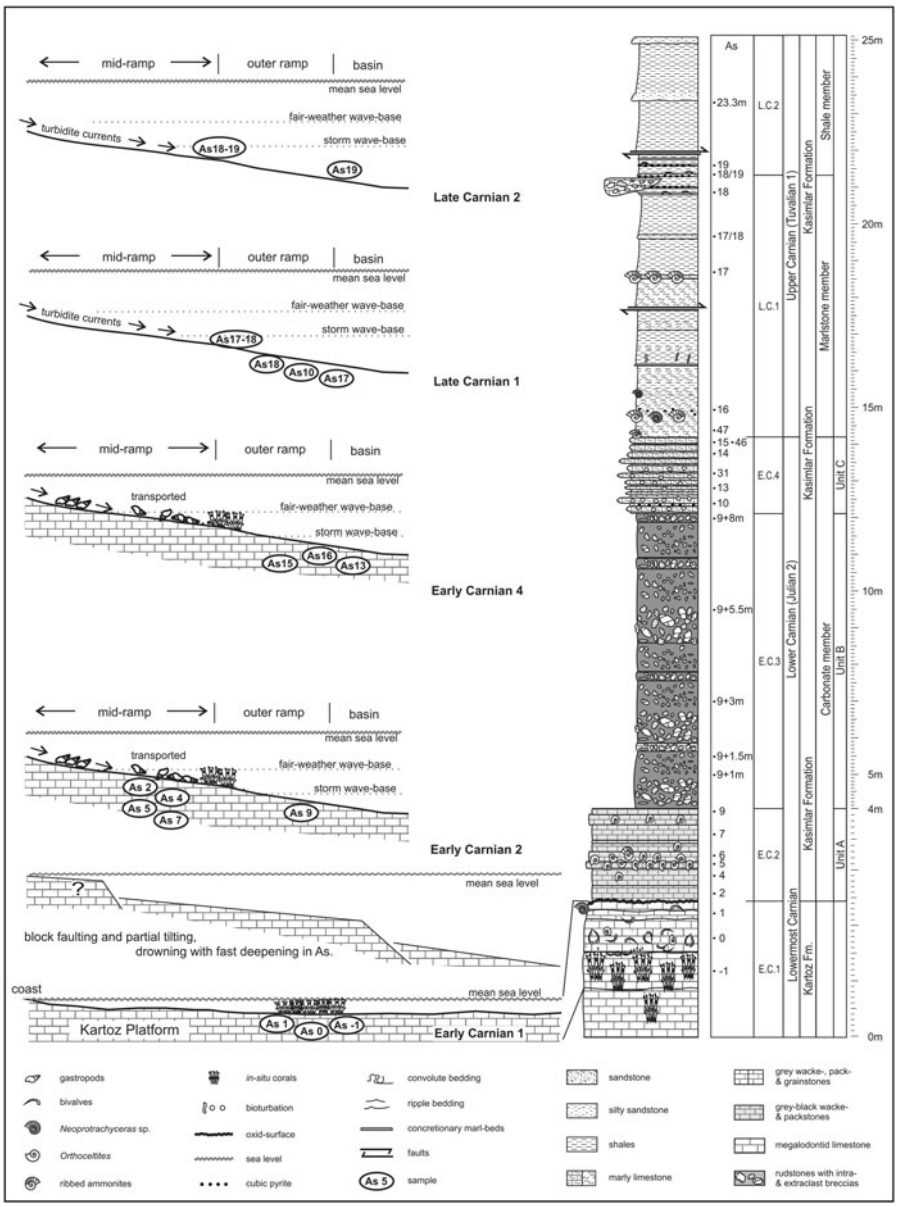

Fig. 3 Log of the section Aşağiyaylabel with indicated stratigraphy, sample positions (As 1–As 19) and speculative depositional sections (not to scale) from the Kartoz Formation (Early Carnian 1) and the Kasımlar Formation (Early Carnian 2–Late Carnian; e.g., Julian–Tuvalian). Please note that the scale changes at 4 m. Indicated depositional areas of the facies types As 1 to As 23.3 m correspond to log and stratigraphy to the right. Topography and suggested position of facies types modified after Flügel (2004)

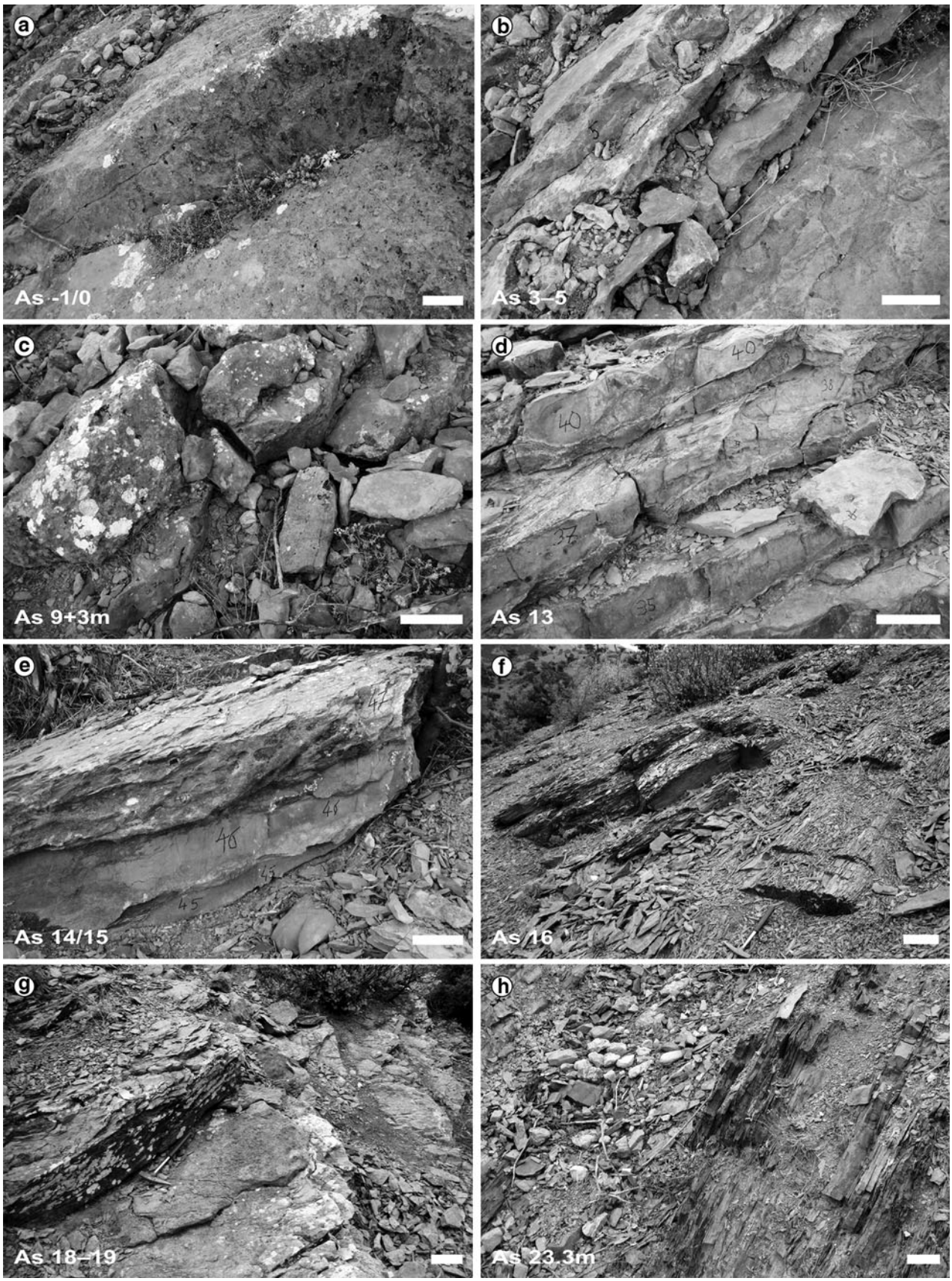
a
As -1/0
b
As 3–5
c
As 9+3m
d
As 13
e
As 14/15
f
As 16
g
As 18–19
h
As 23.3m

Stratigraphic log and biostratigraphy

The section at Aşağiyaylabel comprises about 50 m of essentially calcareous beds passing into marlstones (in part marly limestones) and shaly beds with considerable siliciclastic input at the top. The lowermost part (0–2.4 m; As −1, As 0, As 1; Figs. 3, 4a) is represented by the Kartoz Formation, a Late Triassic (earliest Carnian, Julian 2) light-grey, shallow-water carbonate succession. It comprises corals and thick-shelled bivalves. *Neoprotrachyceras* sp., found in the upper part of bed As 1, dates the upper part of the Formation as Julian 2 (*A. austriacum* Zone). The top of As 1 ends with a corroded and iron-oxide-stained dissolution surface; a hiatus between the top of As 1 and the overlying Kasımlar Formation cannot be excluded.

The overlying Kasımlar Formation (2.4–25 m; As 2 to As 19; Figs. 3, 4b–h) can be divided into three "members": a carbonate member, a marlstone member, and a shale member. The carbonate member starts with dark-grey to black, thin-bedded limestones containing ammonite-rich beds with a nearly monospecific assemblage of *Orthoceltites* (As 2 to As 9; Fig. 4b) and very rare *Sirenites* sp. represented by floatstones of latest Early Carnian age (Julian 2/II). Towards the top thick slump breccias follow; they contain up to meter-sized patch-reef blocks together with small ammonite coquinas and filament-limestone components (4.1–12.1 m; Fig. 4c). The overlying well-bedded (cm–dm thick) peloidal filament-wackestone (12.1–14.2 m; As 10 to As 15, respectively As 46) with Early Carnian conodonts (*Gladigondolella tethydis* and *Metapolygnathus*) and an ammonite fauna dominated by the genera *Neoprotrachyceras* and *Anasirenites* are of latest Early Carnian age (*Anasirenites* level of Julian 2/IIb). The bioturbated matrix (Figs. 3, 4d) contains juvenile halobiid bivalves, sponge spicules, radiolaria, peloids, and planktic crinoids (=*Osteocrinus* sp.). The argillaceous part of the section starts with the following marlstone member. It consists of bioturbated, mostly peloidal filament-packstones, with thin halobiid pavements, gastropods, and ammonites in specific layers (As 47; As 16; As 17; Fig. 3). Between 19.5 m and 21.1 m, thin layers of silty sandstone and arkoses are present (As 17/18, As 18; Fig. 4g). Ammonites (*Pleurotropites, Spirogmoceras*) from As 16 and 17 date the basal part as earliest Late Carnian. At approximately 21.3 m (Fig. 4h), the marlstone member is replaced by the shale member, a thicker sequence of mm-thick, laminated black shales that are rare in biogenic components except for some thin halobiid layers.

Overall, the studied succession represents the latest Early Carnian (Julian 2) to earliest Late Carnian (Tuvalian 1) time interval with an exactly dated Early to Late Carnian boundary.

Materials and methods

A detailed stratigraphic section of the Early to Late Carnian interval was measured and described. Fifty-four thin-sections, collected in 2007 and 2010, of 17 layers were made and used for petrographic studies. The corresponding bed numbers are indicated by the abbreviation As (for Aşağiyaylabel) and the associated bed number (e.g., As 1 = sample from bed 1). Facies were analyzed using a dissecting microscope (Zeiss Discovery V20) with attached digital camera (AxioCam MRc5). Detailed petrographic analyses were done using a petrographic polarization microscope from Leica (Leica DDM4500P) and a digital camera (Leica DFC4420). Sectioning and photographing were done at the Natural History Museum Vienna and the University of Vienna (Department of Petrography).

Facies description

For a detailed facies description see Table 1.

Kartoz Formation

Coral-bafflestone (Fig. 3: 0.0–2.4 m; As −1 to As 1). This facies is characterized by a dense abundance of in situ corals (Fig. 5a) within the first 70 cm, trapped by a cortoid grainstone matrix (Fig. 5b). In addition to in situ corals, thick-shelled in situ bivalves and coquinas with convex-down oriented bivalves are common. Weathering-resistant structures (top of calcite-filled corals) are present at the top of the layers. This section represents an open platform. (Figs. 3, 4a, 5a, b; Table 1).

Kasımlar Formation

The Kasımlar Formation is composed of the following lithological members and units:

- Carbonate member (units A, B, and C),
- Marlstone member, and
- Shale member

Carbonate member: unit A

The Kasımlar Formation starts with bioclastic pelagic wackestones (Fig. 3: 2.4–4.0 m; As 2 to As 9), which were deposited in a deep shelf margin or mid-ramp position (Flügel 2004). The faunal spectrum mirrors two different source areas of the bioclastic input: thin-shelled bivalves (halobiids), which are most common, represent the autochthonous component (deeper shelf margin), whereas the original habitat of the benthic foraminifera (lagenids),

Table 1 Detailed facies description of investigated thin-sections

Lithostratigraphic unit	Level (m)	Biogenic and abiogenic content	Microfacies zone	See Fig.
Kartoz Fm. Carb. member *Sample*: As −1, As 0, As 1 *Age:* Early Carnian	0–2.4	*Biogenic*: in situ corals, bivalves (e.g., megalodonts), crinoids, ammonites; *Abiogenic*: lithoclasts;	Coral-bafflestone; RMF 12 (SMF 7, FZ 5) *Depositional area (Flügel* 2004*)*: Open platform	3, 4a, 5a–b
Kasımlar Fm. Carb. member (Unit A) *Sample*: As 2 *Age*: Early Carnian	2.4–2.7	*Biogenic*: radiolarians, uniserial lagenid foraminifera, thin- (halobiid) and thick-shelled bivalves, gastropods (*Omphaloptycha*-like), ammonites partly filled with micritic sediment; fragments of echinoderms, rare ostracods; *Abiogenic*: plasticlasts;	Bioclastic, pelagic wackesteone/gastropod-/bivalve-floatstone within an autochthonous micritic peloidal matrix; SMF 8 *Depositional area (Flügel* 2004*)*: Deep shelf margin	3, 5c
Kasımlar Fm. Carb. member (Unit A) *Sample*: As 4 *Age*: Early Carnian	2.7–3.0	*Biogenic*: various amounts of thin-shelled bivalves, ammonites, gastropods (*Omphaloptycha*-like), echinoderms (crinoid-ossicles), bioturbation; *Abiogenic*: authigenic pyrite;	Bioclastic, pelagic wackestone/ammonite-floatstone; SMF 8 *Depositional area (Flügel* 2004*)*: Deep shelf margin	3, 4b, 5d
Kasımlar Fm. Carb. member (Unit A) *Sample*: As 5 *Age*: Early Carnian	3.0–3.1	*Biogenic*: thin- and thick-shelled bivalves, ammonites, echinoderms; *Abiogenic*: plasticlasts;	Bioclastic pelagic wackestone/floatstone with pelsparitic matrix; SMF 8 *Depositional area (Flügel* 2004*)*: Deep shelf margin	3, 4b, 5e
Kasımlar Fm. Carb. member (Unit A) *Sample*: As 6 *Age*: Early Carnian	3.1–3.4	*Biogenic*: ammonites (to 90 %), halobiid bivalves cover the ammonite coquina, sponges, gastropods;	Ammonite or *Orthoceltites* packstone; SMF 12 *Depositional area (Flügel 2004)*: Slope to basinal environment	3, 5f
Kasımlar Fm. Carb. member (Unit A) Sample: As 7 *Age*: Early Carnian	3.4–3.7	*Biogenic*: thin-shelled bivalves, gastropods (*Omphaloptycha*-like), ammonites, echinoderms; *Abiogenic*: plasticlasts;	Bioclastic pelagic wackestone/floatstone; SMF 8 *Depositional area (Flügel* 2004*)*: Deep shelf margin	3, 5g
Kasımlar Fm. Carb. member (Unit A) *Sample*: As 9 *Age*: Early Carnian	3.7–4.1	*Biogenic*: thin-shelled bivalves, ammonites, crionoid-ossicles; *Abiogenic*: plasticlasts;	Bioclastic pelagic wackestone, with fine-grained peloidal matrix; RMF 1–3 *Depositional area (Flügel* 2004*)*: Deep shelf margin	3

Table 1 continued

Lithostratigraphic unit	Level (m)	Biogenic and abiogenic content	Microfacies zone	See Fig.
Kasımlar Fm. Carb. member (Unit B) *Sample*: As 9+x to As 9+8 m *Age*: Early Carnian (Julian 2)	4.1–12.1	*Biogenic*: reef building organisms (primarily chaetetids, rare corals), foraminifera, gastropods, bivalves, ammonites; *Abiogenic*: Cipit boulders, breccias composed of components from different environments: platform or shallow-water facies (patch reef blocks), deeper ramp facies, and pelagic basin facies;	Debris flow deposits, containing up to meter-sized patch reef blocks, Cipit boulders, small ammonite coquina, and filaments; RMF – *Depositional area (Flügel 2004)*: Slope	3, 4c, 5h, 6a–f
Kasımlar Fm. Carb. member (Unit C) *Sample*: As 10 *Age*: Early Carnian (Julian 2)	12.3–12.5	*Biogenic*: filaments, peloids, small sized calcitized radiolarians;	Pelagic packstone, with less bioclastic input than As 9; texture consists of small peloids (possibly fecal pellets); RMF 1–3 (FZ1) *Depositional area (Flügel 2004)*: Basinal environment	3, 6g
Kasımlar Fm. Carb. member (Unit C) *Sample*: As 13 *Age*: Early Carnian (Julian 2)	12.7–13.0	*Biogenic*: halobiid bivalves, sponge spicules, radiolarians, peloids, planktic crinoids (*Osteocrinus* sp.);	Pelagic peloidal filament-packstone with bioclasts, similar to As 10; RMF 1–3 *Depositional area (Flügel 2004)*: Basinal environment	3, 4d, 6h
Kasımlar Fm. Carb. member (Unit C) *Sample*: As 15/As 46 *Age*: Early Carnian (Julian 2)	13.9–14.2	*Biogenic*: thin- and thick-shelled bivalves, echinoderm fragments, miliolid foraminifera, sponges, bryozoans;	Pelagic wackestone (matrix: peloidal pack- to grainstone) with intercalations of fine-grained allodapic layers; RMF 4 *Depositional area (Flügel 2004)*: Outer ramp – basinal environment	3, 4e, 7a
Kasımlar Fm. Marlstone member *Sample*: As 16 *Age*: Late Carnian (Tuvalian 1)	at 14.9	*Biogenic*: rare, thin- and thick-shelled bivalves, fragments of echinoderms, peloids, radiolarians, foraminifera, sponge spicule; *Abiogenic*: pyrite crystals of authigenic origin;	Mudstone and strongly bioturbated bioclastic wackestone with pelsparitic matrix; RMF 2–3 *Depositional area (Flügel 2004)*: Outer ramp – basinal environment	3, 4f, 7b
Kasımlar Fm. Marlstone member *Sample*: As 17a *Age*: Late Carnian (Tuvalian 1)	at 18.6	*Biogenic*: rare fossil debris;	Bioclastic wackestone; Background sedimentation to As 17b, containing rare fossil debris; RMF 5 *Depositional area (Flügel 2004)*: Basinal environment	3, 7c
Kasımlar Fm. Marlstone member *Sample*: As 17b *Age*: Late Carnian (Tuvalian 1)	at 18.6	*Biogenic*: bivalves encrusted by fibrous cement, foraminifera, radiolarians;	Bioclastic wackestone, bivalve shell bed within a micritic peloidal matrix; RMF 5 *Depositional area (Flügel 2004)*: Basinal environment	3, 7d

Table 1 continued

Lithostratigraphic unit	Level (m)	Biogenic and abiogenic content	Microfacies zone	See Fig.
Kasımlar Fm. Marlstone member *Sample*: As 17/18 *Age*: Late Carnian (Tuvalian 1)	19.6–19.7	*Biogenic*: fragments of echinoids, bryozoans; *Abiogenic*: resedimented lithoclasts, poorly rounded plagioclase, some quartz, rare glauconite grains;	Coarse-grained, siliciclastic grainstone (arcosic), cemented by a carbonate matrix; RMF — *Depositional area (Flügel 2004)*: Event bed deposited within a basinal environment	3, 7e$_{1-2}$
Kasımlar Fm. Marlstone member *Sample*: As 18 *Age*: Late Carnian (Tuvalian 1)	20.8–20.9	*Biogenic*: abundant thin-shelled bivalves, radiolarians, echinoid fragments, sponges;	Strongly compacted, bioturbated peloidal packstone; RMF 2 *Depositional area (Flügel 2004)*: Outer ramp to basin	3, 7f
Kasımlar Fm. Shale member *Sample*: As 18/19 *Age*: Late Carnian (Tuvalian 1)	21.3–21.4	*Biogenic*: thick-shelled bivalves; *Abiogenic*: cavities filled with debris and bordered with oncolithic crusts;	Siliciclastic breccias and "floating" blocks (up to 40 cm in diameter); RMF 15 *Depositional area (Flügel 2004)*: Mid Ramp	3, 4g, 7g
Kasımlar Fm. Shale member *Sample*: As 19 *Age*: Late Carnian (Tuvalian 1)	21.4–21.7	*Biogenic*: thin-shelled bivalves, foraminifera, ammonites, echinoderms, bioturbation;	Argillaceous burrowed peloidal packstone; RMF 2–3 *Depositional area (Flügel 2004)*: Outer ramp to basin	3, 4g, 7h

RMF 1: Calcisiltite and mudstone with peloids, very fine skeletal debris, sponge spicules, sometimes finely laminated. RMF 2: Argillaceous burrowed mudstone and wackestone; rare agglutinated foraminifera, ostracods, echinoderms. RMF 3: Burrowed bioclastic wackestone and packestone with diverse, common to abundant fossils (bivalves, brachiopods, echinoderms) and peloids. Skeletal grains not worn; whole fossil preservation common. RMF 4: Peloidal wackestone and packstone. RMF 5: Pelagic mudstone with planktonic microfossils and open-marine nektonic fossils (e.g., ammonites). SMF 7: Organic boundstone, platform-margin "reef". SMF 8: Whole fossil wackestone/floatstone. SMF 12: Limestone with shell concentration.—FZ 2: Deep shelf. FZ 5: Platform-margin reefs. FZ1, FZ3, FZ 4 are missing at Aşağiyaylabel

The nomenclature of ramp- and standard microfacies types (RMF/SMF) as well as facies zones (FZ) is adopted from Dunham (1962), Flügel (1972), and Wilson (1975). Carbonate classification follows the nomenclature of Dunham (1962) and Folk (1959, 1962). Eight microfacies types (Figs. 5, 6, 7) were detected. For the detailed position of the different facies, see Figs. 3 and 4

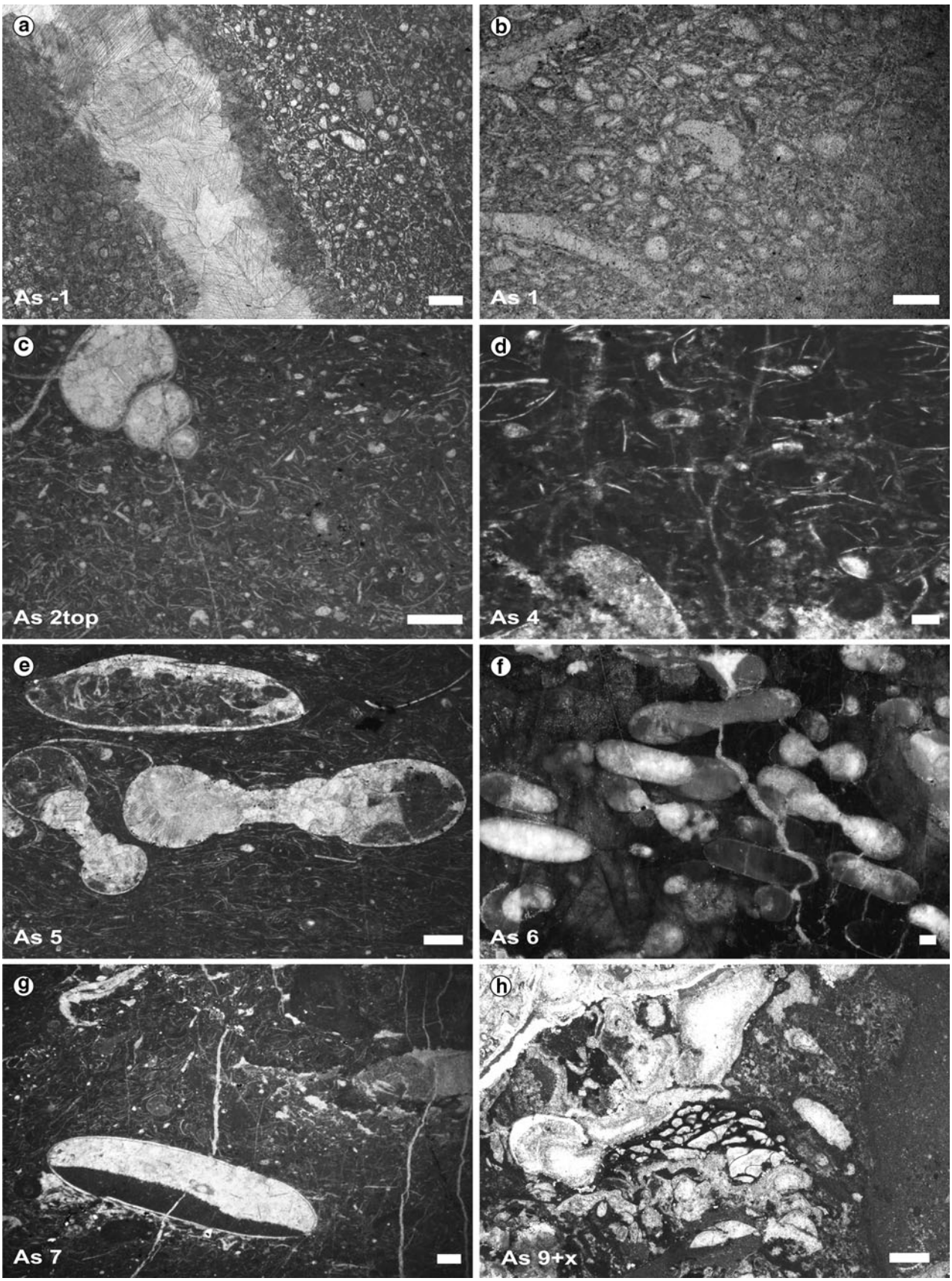
a
As -1
b
As 1
c
As 2top
d
As 4
e
As 5
f
As 6
g
As 7
h
As 9+x

◀ **Fig. 5** Thin-section photographs of facies As −1 to As 9+x. Kartoz Formation: **a** As −1, bioclastic bafflestone with abundant in situ corals trapped by cortoid grainstone matrix. Calcitic in situ coral (*thick whitish structure*). **b** As 1, bioclastic grainstone with abundant grains encrusted by cyanobacteria together with common megalodontid bivalves and echinoderm fragments. Kasımlar Formation: **c** As 2top, bioturbated gastropod-bivalve floatstone with micritic peloidal matrix containing thin-shelled halobiid bivalves. **d** As 4, ammonite-gastropod floatstone with micritic peloidal matrix containing abundant thin-shelled halobiid bivalves. **e** As 5, bioclastic floatstone with abundant ammonites (*Orthoceltites*) and halobiid shells accompanied by rare gastropods. Ammonites and gastropods filled with coarse sparry calcite floating in micritic matrix. **f** As 6, ammonite or *Orthocletites* packstone; densely packed and parallel-arranged, well-preserved ammonite (*Orthoceltites* sp.) shells forming a coquina. **g** As 7, bioclastic floatstone with thin-shelled bivalves (halobiids), gastropods *(Omphaloptycha*-like), abundant ammonites (*Orthoceltites*) filled with coarse sparry calcite, and numerous echinoderm fragments. **h** As 9+x, characteristic sponge-accentuated Cipit facies, rare in corals. All *scale bars* 1 mm

the thick-shelled bivalves (megalodontids), and the large, low-spired gastropods was situated on a fore slope or on a shallow-marine ramp. Tilted geopetal fills of gastropods and ammonites (*Orthoceltites* sp.), together with clasts of eroded semi-lithified sedimentary layers ("plasticlasts"), prove episodic erosion, downward transport, and re-sedimentation. Bioturbation has mostly obliterated the original arrangement of autochthonous fine-grained sediments (together with thin-shelled bivalves and radiolaria) alternating with coarser-grained tempestitic layers. When the original layering is preserved, bedding planes are strongly affected by stylolites (As 4). Common authigenic pyrite (often as well-developed crystals) in different levels of the section (As 4) is probably of synsedimentary origin. However, the high abundance of halobiid bivalves and the dark-colored sediment could point to temporary dysaerobic conditions of the bottom waters and/or the pore-fluids of the unconsolidated sediments (Flügel 2004; McRoberts 2000, 2010). Reddish brown dolomitic spots (As 4) are interpreted as diagenetic overprint during a later emersion phase under arid or semi-arid conditions (Al-Hashimi and Hemingway 1973) (Figs. 3, 4b, 5c–g; Table 1).

Carbonate member: unit B

Mass flow deposits with Cipit-boulders (Fig. 3: 4.0–12.1 m; As 9+x to As 9+8 m).

These probably tectonically induced gravity-flow deposits demonstrate an important turning point in the basin-forming process, which started with down-faulting and block-tilting, accompanied by a steepening of the adjacent slope (Figs. 3, 4c, 5h, 6a–f; Table 1).

Carbonate member: unit C

Pelagic wackestone/packstone with bioclasts (Fig. 3: 12.1–14.2 m; As 10 to As 15).

This part of the section is characterized by a remarkable increase of the proportion of allodapic sediments (As 15). Tempestitic layers with platform-derived material (thick-shelled foraminifera together with rare dasycladacean algae and sponges) alternate with pure mudstones of the background sedimentation, which contain abundant authigenic euhedral pyrite crystals. The "clotted fabric" of the fine-grained "groundmass" (Flügel 1982, p. 119) hints that this matrix was probably originated via decomposition of former peloidal grain-/packstones. The texture of the sediment, which alternates with the allodapic layers, has been strongly affected by pressure solution. Small-sized radiolaria starting at the base of the section (As 10) prove a basinal environment (FZ1, Flügel 1982: tab. 43). The radiolaria are mostly calcified (mould preservation); the original mineralogy and porous wall structure is preserved only in areas that underwent early diagenetic silicification. The presence of thick-shelled bivalves indicates temporary shallowing (Figs. 3, 4d–e, 6g–h, 7a; Table 1).

Marlstone member

Marlstones with calcareous intercalations (14.2–21.3 m; As 16 to As 18).

The lower segment of this section features a shallowing upward tendency. The sequence starts with partly bioturbated bioclastic wackestones and pelsparitic packstones, followed by shales with a 1.1-m-thick intercalation of carbonates (As 17; bioclastic wackestone) with thick-shelled bivalves. A small (10 cm) arkosic sandstone layer (As 17/18) with echinoid and bryozoan fragments is present at the top of the sequence. Crystals of authigenic pyrite are common in different layers of the succession (Figs. 3, 4f, 7b–f; Table 1).

Shale member Shales with limestone intercalations (21.3–25+ m; As 19).

In the sequence at the top, which is exposed above the marlstone member, shales (Fig. 4g–h) with episodic intercalations of thin-bedded carbonates dominate. Samples of two of these intercalated carbonate layers (As 18, As 19) are composed of strongly bioturbated peloidal packstone with thin-shelled bivalves, rare radiolaria, and echinoid fragments (Figs. 3, 4g–h, 7g–h; Table 1).

Facies interpretation

The deepening sequence at Aşağiyaylabel: from the Kartoz Formation to the Kasımlar Formation

Kartoz Formation

The Kartoz Formation is represented by sediments of an open platform, mainly composed of well-sorted cortoid

grainstones with rare bioclasts (As −1, As 0, and As 1; Fig. 5a, b). A 2.4-m-thick layer of a coral bafflestone is intercalated near the top of this sequence. Microscopic vertical fissures extending a few meters below the top of the Kartoz Fm. are partly filled with vadose silt, pointing to at least one episodic period of emersion (Fig. 4a). Remaining open spaces were filled in a second phase (see below). The transgressive pulse of the coral carpet layer probably reflects small-scale sea-level fluctuations. A hardground at the top of the Kartoz Formation indicates a period of non-sedimentation during which pelagic sediment sealed the open karst fissures. This points to a rapid drowning of the shallow-water platform. The boundary between the Kartoz Formation and the overlying Kasımlar Formation is characterized by a sharp change in lithology and facies, probably reflecting a hiatus.

Kasımlar Formation

Carbonate member The Kasımlar Formation starts at 2.4 m with black, 1.5-m-thick limestones marked by densely packed ammonites (*Orthoceltites*) within a micritic matrix. The faunal spectrum (As 2, 4, 5, 6 and 7; Fig. 5c–g) suggests two different source areas of the bioclastic input: thin-shelled bivalves (halobiids), which are the most abundant faunal element, are autochthonous, whereas the original habitat of the thick-shelled bivalves and large, low-spired gastropods was situated on a fore slope or on a shallow-marine ramp. Tilted geopetal fills of gastropods, together with clasts of eroded semi-lithified sedimentary layers ("plasticlasts"), indicate episodic erosion, downward transport, and re-sedimentation. Generally, the assumed original arrangement of autochthonous fine-grained sediments alternating with coarser-grained tempestitic layers is obliterated by bioturbation. Where the original bedding is preserved, tops of the beds are strongly affected by pressure solution (As 4). The gastropods are similar to *Omphaloptycha* (Andrzej Kaim, pers. comm.). The tilted geopetal fills of the ammonite and gastropod shells within As 5 (Fig. 5e) indicate their lithification within another facies and subsequent transport to the final depositional area. The breccia-like bioclastic floatstones (As 2 to As 9; Fig. 5c–g) may be interpreted as distal equivalents of the following 8 m of rudstones with intra- and extraclast breccias (Fig. 3). The genesis of these mass flow breccias seems to be similar to that of the Cipit boulders (Fig. 5h) first described by Richthofen (1860); see also Fürsich and Wendt 1977). Cipit boulders are meter- to tens-of-meters sized isolated blocks embedded in calciturbiditic, volcaniclastic, marly, or argillaceous basinal sediments (Richthofen 1860). The debris flow components of a deeper ramp (Fig. 6a) are positioned next to components of pelagic facies (Fig. 6b) as well as next to shallow-water material (Fig. 6c) and components composed of reef-building organisms (Fig. 6d). Different generations of chaetetids and well-preserved internal sedimentation are visible (Fig. 6e). Similar breccias have been described by Keim and Brandner (2001) and interpreted as indicating extensional synsedimentary tectonics, which leads to scarps, block-tilting, graben structures, and finally to breccia deposition. Sediments and biogenic components of platform margins have thereby been embedded within basinal sediments as gravity-displaced carbonate boulders (Brandner et al. 1991). Sedimentary structures (Fig. 6f) indicate a still plastic or semi-lithified sediment, which underwent further plastic deformation; this sediment originated by the absorption of material from the bedrock during the gravity displacement of the Cipit-like boulders. The tectonically induced gravity-flow deposits are evidence of an important turning point in the basin-forming process, which started with down-faulting, local synsedimentary tectonics, and block-tilting, probably accompanied by a steepening of the adjacent slope. This most likely involved a different geometry of the basin margin as well as another carbonate productivity zone shortly after deposition of the Cipit-like breccias. Through seismic activity, tilting, and down-faulting, a formation of highs in the current basin may be assumed.

This phase ended abruptly and gave way to a deeper-water autochthonous succession of bedded limestones, indicating a basinal environment within the next two meters (As 10, As 46top; Fig. 6g), rich in radiolaria and sponge spicules. This part of the section, however, is characterized by a clear increase in allodapic sediments (As 15, As 31; Fig. 7a). Productive carbonate platform relicts are indicated by a characteristic, well-preserved (not corroded and/or fragmented) biogenic content (shallow-water- and reef-building-organisms: Dasycladacea, chaetetids, calcareous sponges, gastropods) and layers of shallow-water-derived material. There are no indications that the

Fig. 6 Thin-section photographs of different facies components of debris flow deposits (carbonate member unit B) and pelagic packstones of the carbonate member unit C. **a** As 9+1 m, component containing material from the deeper ramp. **b** As 9+1.5 m, component representing pelagic facies. **c** As 9+3 m, component composed of material derived from shallow water. **d** As 9+8 m, component containing reef-building organisms (e.g., chaetetid sponge). **e** As 9+zD, component containing different generations of chaetetids and well-preserved internal sedimentation. **f** As 9+5.5 m, component representing sedimentation structures indicating plastic deformation of semi-lithified sediment: an excellent example for absorption from the bedrock. **g** As 10, pelagic packstone with bioclasts, matrix consisting of small peloids (perhaps fecal pellets of halobiid bivalves) with filaments (halobiids), sponge spicules, and radiolaria. **h** As 13, pelagic packstone with bioclasts, bioturbated matrix with bioturbation containing halobiid bivalves, sponge spicules, radiolaria, peloids, planktic crinoids (=*Osteocrinus* sp.?). Detailed description of thin-sections in text. All *scale bars* 1 mm

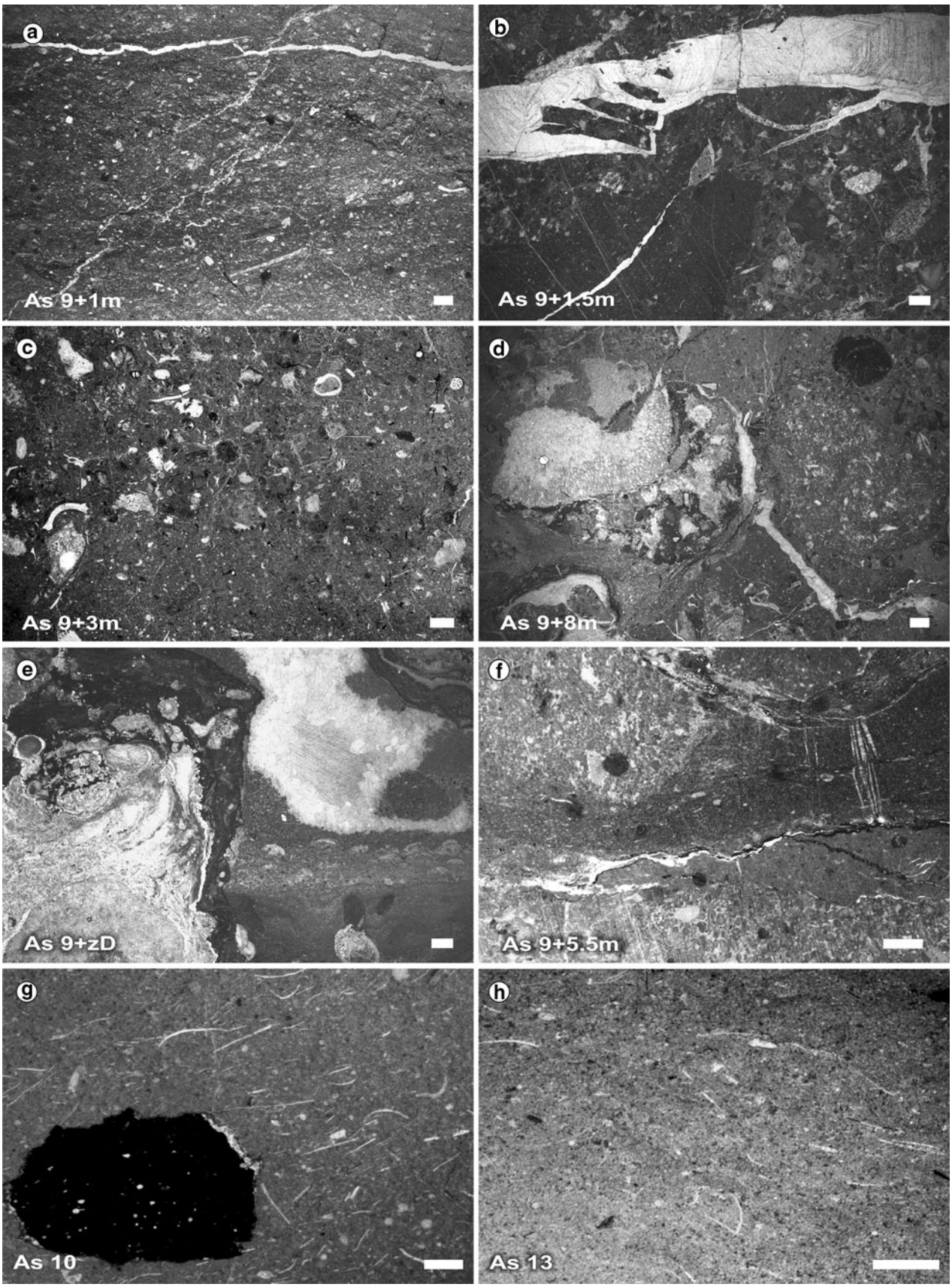
a
As 9+1m
b
As 9+1.5m
c
As 9+3m
d
As 9+8m
e
As 9+zD
f
As 9+5.5m
g
As 10
h
As 13

shallow-water material represents reworked Kartoz Platform material, nor is there evidence for a strong subaerial alteration. We therefore interpret this material as having been transported from a contemporaneous marginal area into the basin. The fine-grained texture (As 10 and As 13; Fig. 6g–h) consists of small pellets, most probably derived from halobiid bivalves. The recognized global major appearance of osteocrinoids within Ladinian to Carnian strata (Kristan-Tollmann 1970) agrees with occurrences of *Osteorcinus* within sample As 13 of Aşağiyaylabel. At the top of As 46, a layer of thin-shelled pelagic bivalves was detected. The same facies is represented within As 47. Although thin-shelled pelagic bivalves characterize this facies, many other calcitic biogenes (e.g., echinoderms, thick-shelled foraminifera together with rare dasycladacean algae and sponges) are also present. The parallel arrangement of the bivalves indicates current control. Tempestitic layers with platform-derived material alternate with pure mudstones of the background sedimentation (As 15); these mudstones contain abundant euhedral pyrite crystals of authigenic origin. The "clotted fabric" of the fine-grained "groundmass" (Flügel 1982, p. 119) hints that the observed matrix probably originated via decomposition of former peloidal grain-/packstone. The texture of the sediment, which alternates with the allodapic layers, is strongly affected by pressure solution. The radiolaria skeletons are mostly calcified. Thick-shelled bivalves indicate a temporary shallowing.

Marlstone member The Upper Carnian (Tuvalian 1) is represented by calcareous marls to subordinate marlstones alternating between sediments poor in fossils, except for distinct layers rich in halobiid shells and ammonites (As 47 to As 18/19; Fig. 7b–g); Fig. 7a–h). The lower part of this interval shows a shallowing-upward tendency. The sequence starts with partly bioturbated bioclastic wackestones and pelsparitic packstones, followed by calcareous marls. The macro-invertebrate fauna of the Tuvalian 1 unit is sparse, except for one *Pleurotropites* layer (As 17; Fig. 3) and some halobiid coquinas (*Halobia*, As 18 to As 19; Fig. 3, 7f, h). Such coquinas occur in deep-water, oxygen-deficient settings as well as in "pelagic" or "filamentous" limestones, which represent fully oxygenated marine settings (e.g., Hallstatt facies; McRoberts et al. 2008; McRoberts 2000, 2010). Crystals of authigenic pyrite are common in several layers of the succession (As 16, As 18; Fig. 3, 7b, f). Thin-section As 17 represents a bioclastic wackestone with thick-shelled bivalves (Fig. 7c–d). A small (10 cm) arkosic sandstone layer with echinoid and bryozoan fragments occurs near the top of the sequence (As 17/18; Fig. 7e).

Shale member This member consists of shales with rare, thin carbonate interbeds. One sample of these (As 19; Fig. 7h) is composed of strongly bioturbated peloidal packstone with thin-shelled bivalves, rare radiolarians, and echinoid fragments. Apart from the mentioned sandstone layer, another coarse-grained bed occurs at approximately 21 m (As 18/19; Figs. 4g, 7g); it is composed of an intraformational slump breccia. Subangular boulders are embedded in a brownish-yellow, fine-grained limestone matrix whose color originates from oxidation of pyrite. The light-colored angular breccia components are apparently derived from a shallow-water margin of the Kasımlar Basin. Nonetheless, as no such contemporaneous facies exists in the basin, we interpret this breccia to represent reworked material from the Kartoz Formation.

Fig. 7 Thin-section photographs of facies As 15 to As 19. Kasımlar Formation: **a** As 15, pelagic peloidal pack- to grainstone with biogenic components of dasycladacean green algae, sponge spicules, crinoids, thin- and thick-shelled bivalves (halobiids), miliolid foraminifera, and bryozoans. **b** As 16, strongly bioturbated, fine bioclastic wackestone with biogenic components such as thin- and thick-shelled bivalves, fragments of echinoids, peloids, radiolaria, foraminifera, and sponge spicules. **c** As 17a, bivalve wacke- and floatstone containing rare biogenic components such as thin-shelled bivalves (halobiids), foraminifera, and radiolaria. **d** As 17b, bivalve wacke- and floatstone with abundant bivalve shells (encrusted by fibrous cementation) floating within a micritic peloidal matrix with foraminifera and radiolaria. **e_1** As 17/18, arkose composed of poorly rounded components, mostly re-sedimented lithoclasts containing biogenic components such as fragments of echinoids and bryozoans, plagioclase, quartz grains, and rare glauconite, cemented by a carbonate matrix. **e_2** As 17/18, same sample as **e_1**, shown under a petrographic polarization microscope. **f** As 18, strongly compacted, bioturbated peloidal packstone with abundant thin-shelled bivalves (*halobiids*), radiolaria, echinoid fragments, and sponge spicules, with signs of bioturbation, stylolithic structures, and large pyrite crystals (1–3 mm) coated by calcite cement. **g** Slip breccia, (=same horizon as As 18/19) containing different reworked components and framboidal pyrites. **h** As 19, argillaceous, bioturbated peloidal packstone with abundant thin-shelled bivalves (*halobiids*), rare ammonites, radiolaria, echinoid-fragments, and sponge spicules, with signs of bioturbation, stylolithic structures, and abundant large pyrite crystals (1–3 mm) coated by calcite cement. Detailed description of thin-sections in text. All *scale bars* 1 mm

Discussion

Aşağiyaylabel and the Carnian Pluvial Episode

As noted by Hallam (1996) and Hornung (2008), the CPE was marked by a major facies change from a carbonate-dominated to an argillaceous-dominated sedimentary regime. This phase was also characterized by a major decrease in marine and epicontinental faunas, as seen in many marine invertebrate groups and terrestrial elements such as tetrapods (Hallam 1996; Hornung 2008). The most affected faunas were shallow-water inhabitants (reef builders) of the Tethyan-wide reefs and platforms. This Tethys-wide demise of reef systems and carbonate

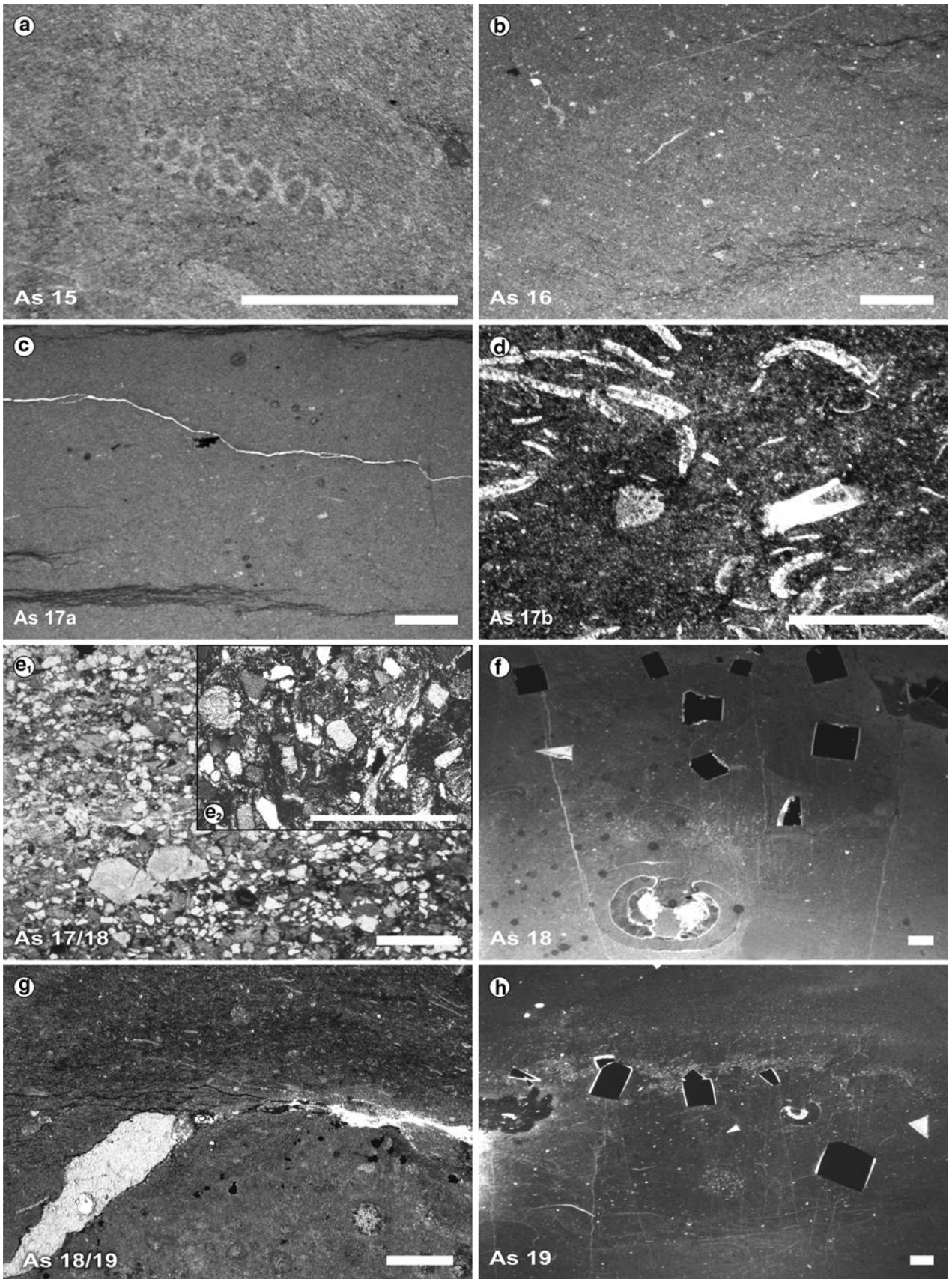
a
As 15
b
As 16
c
As 17a
d
As 17b
e1
e2
As 17/18
f
As 18
g
As 18/19
h
As 19

platforms is dated to the late Julian 1 (Hornung and Brandner 2005; Hornung et al. 2006, 2007a, b). Multistratigraphic studies concluded that this demise was synchronous throughout the Tethys area within the *Metapolygnathus carnicus* conodont range zone and the late *T. aonoides* ammonite zone (Hornung 2008). In contrast to the western Tethys, where the turnover occurred within the Early Carnian, in the Taurus Mountains (Aşağiyaylabel) the sedimentation remains carbonate-dominated and becomes terrigenous only at the base of the Late Carnian; this corresponds to the boundary between the limestone and the marlstone member of the Kasımlar Formation. These two members are therefore, despite their facial identity, younger than the Early Carnian Alpine Reingraben Shales (Hornung and Brandner 2005) or *Halobia* Shales of northern Turkey (Yurttas-Özdemir 1973) and the Rama Fm. of the Indian Himalaya, respectively (Hornung et al. 2006, 2007a, b). Only in the Lagonegro Basin in the southern Apennines (southern Italy) does an interval of green shales and radiolarites (lacking carbonate deposits) correspond in time to the turnover at Aşağiyaylabel. It is interpreted there as a shallowing of the carbonate compensation depth and again as a result of the CPE (Rigo et al. 2007).

The mechanism triggering the CPE is still under debate. Generally accepted is that global warming (caused by the rifting of Pangea) enhanced humidification, triggering climate change during the Early Carnian (Hornung et al. 2006, 2007a, b; Hornung 2008). Strong humidification by enhanced monsoonal phases led to increased freshwater runoff and enhanced nutrification of the Tethyan Ocean (Simms and Ruffell 1989; Hornung et al. 2007a, b), destroying reefs and platforms and reducing nektonic biodiversity. Within the studied section, an outstanding feature is the abrupt facies change but increased carbonate productivity during the Early Carnian (Julian 2). As we have no evidence for terrestrial input during this time interval, the poor nutrient availability probably led to an increased carbonate accumulation rate (Hallock and Schlager 1986). Such a negative correlation between nutrient supply and carbonate productivity suggests poor paleocirculation (De Boer et al. 2006). An important result of the present study is the distinctly time-delayed facies change from a carbonate to an argillaceous sedimentation in Aşağiyaylabel. While most sequences of the western Tethys show a turnover within the Early Carnian, the succession in Turkey and the deposits of the Lagonegro Basin are clearly at the Julian–Tuvalian boundary, at least 2 Ma later. Interestingly, this turnover coincides with an extinction event affecting many pelagic taxa of ammonites and conodonts (Krystyn 1983, 1991; Rigo et al. 2007; Hornung et al. 2007a, b). According to Stampfli et al. (2002) and Moix et al. (2008), the paleolatitude of Turkey (about 7° N; Fig. 1a) and the Lagonegro Basin (about 8–9° N, Fig. 1a) was closer to the equator than the South- and Austroalpine segments (about 17° N) of the northern Tethys or the Himalaya (at least 30° S). Muttoni et al. (2004) provide an analogous reconstruction, although with a 10° northward shift. We therefore assume that higher latitudes could play an important role by causing an earlier sedimentary turnover. Facies changes at Aşağiyaylabel mirror a coupling effect of lower paleogeographic latitudes (Krystyn 1983, 1991; Rigo et al. 2007; Hornung et al. 2007a, b) accompanied by Tethyan-wide climate changes during the CPE.

Conclusions

The studied outcrop at Aşağiyaylabel represents a late Triassic drowning succession marked, like most Tethyan Carnian sequences, by a facies change from carbonates (carbonate platform, patch reefs, hemipelagic limestones) to argillaceous sediments (marlstones, shales). The base of the succession is characterized by a sudden drowning of a carbonate platform followed directly by deeper-water limestones. Synsedimentary tectonics probably triggered the drowning of the Kartoz platform, which led to down-faulting and tilting of the platform and to a new basin geometry along a deeper ramp setting. The fine-grained autochthonous microfacies of the deeper-water limestones suggests a low-energy bottom environment with episodic, current-induced input of coarser-grained tempestitic layers, now obliterated by bioturbation. The pelagic filament (halobiid bivalve) facies is mixed with allochthonous biogenic material (e.g., thick-shelled bivalves, gastropods; also plasticlasts) from the fore-slope or shallow-marine ramp. This points to different source areas of the bioclasts. Synsedimentary unrest is recorded by punctuated redeposition of shallow-water material of reefal and interior ramp origin in the form of breccias and detrital interbeds. These components help to reconstruct the original zonation and differentiation within the ramp; they indicate continuation of reef-favorable conditions until the end of the Early Carnian, when another major sedimentary change led to siliciclastic-dominated sedimentation. The change at the beginning of the Late Carnian to marly and later on to shaly sedimentation is interpreted to reflect climate change due to more humid conditions.

We consider the main litho-change from carbonates to siliciclastic sediments, which at Aşağiyaylabel took place at least 2 Ma later than along the northwestern Tethyan margin, as a similar but diachronous expression of the common late Early Carnian carbonate and reef demise episode. Aşağiyaylabel shares this late turnover to siliciclastic sedimentation with the Lagonegro Basin (Southern Apennines), both of which are ascribed to equatorial

Triassic paleolatitudes (approximately 9° N). This leads us to conclude that humidity-driven siliciclastic sedimentation of the so-called Carnian Pluvial Episode probably started earlier at higher paleolatitudes (Alps approximately 17-25° N, Himalaya 30° S) than in equator-near successions. Additional investigations are needed to clarify the time-shift of the major sedimentary change (approx. 2 my) at Aşağiyaylabel. Here, the sedimentary changes are apparently linked more to different coupling effects and a subsequent climate change than to a single climatic event.

Acknowledgments This study was funded by project P 22109-B17 of the Austrian Science Fund (FWF). The authors highly appreciate the help and support from the Turkish Geological Survey (MTA) and are thankful for the digging permission within the investigated area. We thank Helga Zeitlhofer (University of Vienna) for help with polarization microscope analysis. Crinoids were determined by Andreas Kroh (Natural History Museum Vienna) and gastropods by Andrzej Kaim (Instytut Paleobiologii PAN, Warsaw, Poland). Franz Topka (Natural History Museum Vienna) assisted in sampling and preparing the ammonite specimens. Anton Englert (Natural History Museum Vienna) prepared the thin-sections. We kindly acknowledge Rainer Brander and an anonymous reviewer for their comments, which greatly improved the quality of this manuscript. We are also extremely grateful to the editor of FACIES, Franz T. Fürsich, for his encouragement and helpful comments.

References

Aigner T, Bachmann GH (1992) Sequence stratigraphic framework of the German Triassic. Sediment Geol 80:115–135

Al-Hashimi WS, Hemingway JE (1973) Recent dedolomitization and the origin of the rusty crusts of Northumerland. J Sediment Petrol 43:82–91

Andrew T, Robertson A (2002) The Beyşehir-Hoyran-Hadim nappes: genesis and emplacement of Mesozoic marginal and oceanic units of the northern Neotethys in southern Turkey. J Geol Soc Lond 159:529–543

Brandner R, Flügel E, Senowbari-Daryan B (1991) Microfacies of carbonate slope boulders: indicator of the source area (Middle Triassic: Mahlknecht Cliff, Western Dolomites). Facies 25:279–296

De Boer PL, Harting M, Mueller A, Van der Zwan KL (2006) Distinction between black shales formed in high-productivity and in stagnant-basin settings (abstr.). Am Geophys Union Fall Meeting 2006: #PP41B-1198

Dercourt J, Ricou LE, Vrielynck B (1993) Atlas Tethys palaeoenvironmental maps. Gaulthier-Villars, Paris, p 307

Dercourt J, Gaetani M, Vrielynck B, Barrier E, Biju-Duval B, Brunet MF, Cadet JP, Crasquin S, Sandulescu M (eds) (2000) Atlas Peri-Tethys—Palaeogeographical maps. Commission of the Geological Map of the World, Paris, p 269

Dumont JF (1976) Etudes géologiques dans les Taurides Occidentales: Les formations paléozoiques et mésozoiques de la coupole de Karacahisar (Province d'Isparta, Turquie). Dissertation, University of South Paris, p 213

Dumont JF, Kerey E (1975) Kırkavak Fayı [The Kırkavak Fault]. Tür Jeol Kurumu Bül 18:59–62

Dunham RJ (1962) Classification of carbonate rocks according to their depositional texture. In: Ham WE (ed) Classification of carbonate rocks—a symposium. Am Assoc Petrol Geol Mem 1:108–121

Flügel E (1972) Mikrofazielle Untersuchungen in der alpinen Trias: Methoden und Probleme. Mitt Ges Geol Bergbaustud 21:9–64

Flügel E (1982) Microfacies analysis of limestones. Springer, Berlin, p 633

Flügel E (2004) Microfacies of carbonate rocks. Springer, Berlin, p 976

Flügel E, Senowbari-Daryan B (2001) Triassic reefs of the Tethys. In: Stanley GD Jr (ed) The history and sedimentology of ancient reef systems. Kluwer Academic/Plenum Publisher, New York, pp 217–249

Folk RL (1959) Practical petrographic classification of limestones. Am Assoc Petrol Geol Bull 43:1–38

Folk RL (1962) Spectral subdivision of limestone types. In: Ham WE (ed) Classification of carbonate rocks—a symposium. Tulsa, OK, Am Assoc Petrol Geol Mem 1:62–84

Fürsich FT, Wendt J (1977) Biostratinomy and palaeoecology of the Cassian formation (Triassic) of the Southern Alps. Palaeogeogr Palaeoclimatol Palaeoecol 22:257–323

Gallet Y, Krystyn L, Marcoux J, Besse J (2007) New constraints on the End-Triassic (Upper Norian–Rhaetian) magnetostratigraphy. Earth Planet Sci Lett 255:458–470

Gianolla P, Ragazzi R, Roghi G (1998) Upper Triassic amber from the Dolomites (northern Italy) a paleoclimatic indicator? Riv Ital Paleontol Stratigr 104:381–390

Gindl A (2000) Paläoökologie triassischer Ammonitenfaunen des Taurusgebirges (Türkei). Unpublished Diploma thesis, University of Vienna, p 80

Golonka J (2004) Plate tectonic evolution of the southern margin of Eurasia in the Mesozoic and Cenozoic. Tectonophysics 381:235–273

Göncüoglu CM, Sayit K, Tekin UK (2010) Oceanization of the northern Neotethys: geochemical evidence from ophiolitic melange basalts within the İzmir–Ankara suture belt, NW Turkey. Lithos 116:175–187

Gradstein FM, Ogg JG, Smith AG (2004) A geologic time scale 2004. Cambridge University Press, Cambridge, p 589

Gutnic M, Monod O, Poisson A, Dumont JF (1979) Géologie des Taurides Occidentales (Turquie). Mém Soc Géol Fr 137:1–112

Hallam A (1996) Major bio-events in the Triassic and Jurassic. In: Walliser OH (ed) Global events and event-stratigraphy. Springer, Berlin, pp 265–283

Hallam A, Wignall PB (1997) Mass extinctions and their aftermath. Oxford University Press, Oxford, p 330

Hallock P, Schlager W (1986) Nutrient excess and the demise of coral reefs and carbonate platforms. Palaios 1:389–398

Hochuli A, Frank SM (2000) Palynology (dinoflagellate cysts, spore-pollen) and stratigraphy of the Lower Carnian Raibl Group in the Eastern Swiss Alps. Eclogae geol Helv 93:429–443

Hornung T (2008) A Tethys-wide mid-Carnian (Upper Triassic) carbonate productivity crisis: evidence for the Alpine Reingraben Event from Spiti (Indian Himalaya ?). In: Hornung T (ed) The Carnian Crisis in the Tethys Realm. Multistratigraphic studies and palaeoclimate constraints. VDM Verlag Dr. Müller, Saarbrücken, p 237

Hornung T, Brandner R (2005) Biochronostratigraphy of the Reingraben Turnover (Hallstatt Facies Belt): local black shale events controlled by regional tectonics, climatic change and plate tectonics. Facies 51:475–494

Hornung T, Krystyn L, Brandner R (2006) A Tethys-wide mid-Carnian (Upper Triassic) carbonate productivity decline: evidence for the Alpine Reingraben Event from Spiti (Indian Himalaya). J Asian Earth Sci 30:285–302

Hornung T, Spatzenberger A, Joachimsky MM (2007a) Multistratigraphy of condensed ammonite beds of the Rappoltstein (Berchtesgaden, Southern Germany): unravelling palaeo-environmental conditions on 'Hallstatt deep swells' during the Reingraben Event (late Lower Carnian). Facies 53:267–292

Hornung T, Brandner R, Krystyn L, Joachimsky MM, Keim L (2007b) Multistratigraphic constraints on the NW Tethyan "Carnian Crisis". NM Mus Nat Hist Sci Bull 4:9–67

Keim L, Brandner R (2001) Facies interfingering and synsedimentary tectonics on late Ladinian—early Carnian carbonate platforms (Dolomites, Italy). J Earth Sci (Geol Rundsch) 90:813–830

Keim L, Brandner R, Krystyn L, Mette W (2001) Termination of carbonate slope progradation: an example from the Carnian of the Dolomites, northern Italy. Sediment Geol 143:303–323

Kozur HW (1989) Significance of events in conodont evolution for the Permian and Triassic stratigraphy. Cour Forschinst Senckenb 117:385–408

Kozur HW, Bachmann GH (2010) The middle Carnian Wet Intermezzo of the Stuttgart Formation (Schilfsandstein), Germanic Basin. Palaeogeogr Palaeoclimatol Palaeoecol 290:107–119

Kristan-Tollmann E (1970) Die Osteocrinusfazies, ein Leithorizont von Schwebcrinoiden im Oberladin: Unterkarn der Tethys. Erdöl Kohle 23:781–789

Krystyn L (1983) Das Epidaurus-Profil (Griechenland): ein Beitrag zur Conodonten-Standardzonierung des tethyalen Ladin und Unterkarn. Schr Erdwiss Komm Österr Akad Wiss 5:231–258

Krystyn L (1991) Die Fossillagerstätten der alpinen Trias. Exkursionsführer, pp 23–78

Krystyn L, Gallet Y, Besse J, Marcoux J (2002) Integrated Upper Carnian to Lower Norian biochronology and implications for the Upper Triassic magnetic polarity time scale. Earth Planet Sci Lett 203:343–351

McRoberts CA (2000) A primitive *Halobia* (Bivalvia: Halobioidea) from the Triassic of northeast British Columbia. J Paleontol 74:599–603

McRoberts CA (2010) Biochronology of Triassic bivalves. In: Lucas SG (ed) The Triassic timescale. Geol Soc Lond Spec Publ 334:201–219

McRoberts CA, Krystyn L, Shea A (2008) Rhaetian (Late Triassic) *Monotis* (Bivalvia: Pectinoida) from the eastern Northern Calcareous Alps (Austria) and the end-Norian crisis in pelagic faunas. Palaeontology 51:721–735

Moix P, Beccaletto L, Kozur HW, Hochard C, Rosselet F, Stampfli G (2008) A new classification of the Turkish terranes and sutures and its implication for the paleotectonic history of the region. Tectonophysics 451:7–39

Monod O (1977) Recherches géologiques dans le Taurus Occidental au sud de Beyşehir (Turquie). Dissertation, University of South Paris, p 442

Muttoni G, Kent D, Olsen PE, Stefano PD, Lowrie W, Bernasconi SM, Hernández FM (2004) Tethyan magnetostratigraphy from Pizzo Mondello (Sicily) and correlation to the Late Triassic Newark astrochronological polarity time scale. Geol Soc Am Bull 116:1043–1058

Ogg JG, Ogg G, Gradstein FM (2008) The concise geologic time scale. Cambridge University Press, Cambridge, p 177

Özgül N, Arpat E (1973) Structural units of Taurus orogenic belt and their continuation in the neighbouring regions. Geol Soc Greece Bull 10:156–164

Poisson A (1977) Recherches géologiques dans les Taurides occidentals (Turquie). Dissertation, University of South Paris, p 759

Richthofen FV (1860) Geognostische Beschreibung der Umgebung von Predazzo, Sanct Cassian und der Seisser Alpe in Süd Tyrol. Justus Perthes Verlag, Gotha, p 327

Riedel P (1991) Korallen in der Trias der Tethys: Stratigraphische Reichweiten, Diversitätsmuster, Entwicklungstrends und Bedeutung als Rifforganismen. Mitt Ges Geol Bergbaustud 37:97–118

Rigo M, Preto N, Roghi G, Tateo F (2007) A rise in the carbonate compensation depth of western Tethys in the Carnian (Late Triassic): deep-water evidence for the Carnian Pluvial Event. Palaeogeogr Palaeoclimatol Palaeoecol 246:188–205

Robertson AHF (1993) Mesozoic-Tertiary sedimentary and tectonic evolution of Neotethyan carbonate platforms, margins and small ocean basins in the Antalya Complex, southwest Turkey. Spec Publ Int Assoc Sedimentol 20:415–465

Robertson AHF (2000) Mesozoic-Tertiary tectonic-sedimentary evolution of a south Tethyan Oceanic Basin and its margins in southern Turkey. Geol Soc Lond Spec Publ 173:97–138

Robertson AHF, Poisson A, Akıncı Ö (2003) Developments in research concerning Mesozoic- Tertiary Tethys and neotectonics in the Isparta Angle, SW Turkey. Geol J 38:195–234

Roghi G (2004) Palynological investigations in the Carnian of the Cave del Predi area (Julian Alps, NE Italy). Rev Palaeob Palynol 132:1–35

Rüffer T, Zamparelli V (1997) Facies and biota of Anisian to Carnian carbonate platforms in the Northern Calcareous Alps (Tyrol and Bavaria). Facies 37:115–136

Schlager W, Schöllnberger W (1974) Das Prinzip stratigraphischer Wenden in der Schichtfolge der Nördlichen Kalkalpen. Mitt Geol Ges Wien 66(67):165–193

Scotese CR (1998) Quicktime computer animations. PALEOMAP Project, Department of Geology. University of Texas at Arlington, Arlington

Scotese CR (2001) Paleomap Project, http://www.scotese.com/ (July 2001)

Scotese CR, Gahagan LM, Larson RL (1989) Plate tectonic reconstructions of the Cretaceous and Cenozoic ocean basins. In: Scotese CR, Sager WW (eds) Mesozoic and Cenozoic plate reconstructions. Elsevier, Amsterdam, pp 27–48

Senel M (1997) Türkiye Jeoloji Haritalari, Nr. 4, Isparta Paftasi, Jeoloji Etütleri Dairesi, Ankara 23

Şengör AMC, Yılmaz Y (1981) Tethyan evolution of Turkey: A plate tectonic approach. Tectonophysics 75:181–241

Şengör AMC, Yılmaz Y, Sungurlu O (1984) Tectonics of the Mediterranean Cimmerids: nature and evolution of the western termination of Paleo-Tethys. Geol Soc Lond Spec Publ 17:77–112

Simms MJ, Ruffell AH (1989) Synchronicity of climate change and extinctions in the Late Triassic. Geology 17:265–268

Simms MJ, Ruffell AH, Johnson ALA (1995) Biotic and climatic changes in the Carnian (Triassic) of Europe and adjacent areas. In: Fraser NC, Sues HD (eds) In the shadow of the dinosaurs. Early Mesozoic tetrapods. Cambridge University Press, Cambridge, pp 352–365

Stampfli GM, Borel GD (2002) A plate tectonic model for the Paleozoic and Mesozoic constrained by dynamic plate boundaries and restored synthetic oceanic isochrons. Earth Planet Sci Lett 196:17–33

Stampfli GM, Borel GD, Marchant R, Mosar J (2002) Western Alps geological constraints on western Tethyan reconstructions. J Virtual Explor 8:77–106

Tekin UK, Göncüoğlu C (2007) Discovery of the oldest (Upper Ladinian to Middle Carnian) radiolarian assemblages from the Bornova Flysch zone in Western Turkey: implications for the evolution of the Neotethyan İzmir–Ankara Ocean. Ofioliti 32:131–150

Tekin UK, Göncüoğlu C, Turhan N (2002) First evidence of Late Carnian radiolarians from the Izmir–Ankara suture complex, central Sakarya, Turkey: implications for the opening age of the Izmir–Ankara branch of Neo-Tethys. Geobios 35:127–135

Tollmann A (1976) Analyse des klassischen nordalpinen Mesozoikums: Stratigraphie, Fauna und Fazies der Nördlichen Kalkalpen. Monographie der Nördlichen Kalkalpen 2. Franz Deuticke, Wien, p 580

Wilson JL (1975) Carbonate facies in geologic history. Springer, Berlin, p 471

Yurttaş-Özdemir Ü (1973) Über den Schieferton mit *Halobia* der Halbinsel Kocaeli. Bull Miner Res and Explor Inst Turk (Foreign Edition) 80:43–49